Available online at www.sciencedirect.com
SCIENCE DIRECT®
ELSEVIER
International Journal of Solids and Structures 41 (2004) 6291–6315
INTERNATIONAL JOURNAL OF SOLIDS and STRUCTURES
www.elsevier.com/locate/ijsolstr

Energetically consistent boundary conditions for electromechanical fracture

Chad M. Landis *

Department of Mechanical Engineering and Materials Science, MS 321, Rice University, P.O. Box 1892, Houston, TX 77251-1892, USA

Received 9 December 2003; received in revised form 25 May 2004
Available online 2 July 2004

Abstract

Energetically consistent crack face boundary conditions are formulated for cracks in electromechanical materials. The model assumes that the energy of the solid can be computed from standard infinitesimal deformation theory and that the opening of the crack faces creates a capacitive gap that can store electrical energy. The general derivation of the crack face boundary conditions is carried out for non-linear but reversible constitutive behavior of both the solid material and the space filling the gap. It is shown that a simple augmentation of the *J*-integral can be used to determine the energy release rate for crack advance with these boundary conditions. The energetically consistent boundary conditions are then applied to the Griffith crack problem in a polar linear piezoelectric solid and used to demonstrate that the energy release rate computed near the crack tip is equivalent to the total energy release rate for the solid-gap system as computed from global energy changes. A non-linear constitutive law is postulated for the crack gap as a model for electrical discharge and the effects of the breakdown field on the energy release rate are ascertained.

Keywords: Piezoelectricity; Polarized material; Electrical discharge; Griffith crack; Boundary conditions; Energy release rates

1. Introduction

A significant body of work has appeared in the last few decades on the fracture mechanics of linear piezoelectric materials. Thorough reviews of the literature can be found in McMeeking (1999), Zhang et al. (2001) and Chen and Lu (2002). A point of contention among differing modeling approaches is the crack face boundary condition for the so-called "insulating" crack problem. Herein, three approaches have received considerable attention, (1) the impermeable crack model, (2) the permeable or "closed" crack model,

* Corresponding author. Tel.: +1-713-348-3609; fax: +1-713-348-5423.
E-mail address: landis@rice.edu (C.M. Landis).

0020-7683/$ - see front matter © 2004 Elsevier Ltd. All rights reserved.
doi:10.1016/j.ijsolstr.2004.05.062

and (3) the "exact" boundary conditions. When a cracked body is subjected to certain combinations of mechanical and electrical loads the crack faces will open and usually some type of fluid (usually air) will fill the void. Since the dielectric permittivity of air is much smaller than that of most piezoelectric ceramics of technological interest, the impermeable crack model approximates the permittivity of the gap as zero. This implies that the crack gap does not support any electric displacement, and continuity of electric displacement at the crack surfaces implies that the normal component of electric displacement on the crack surfaces must vanish. In contrast, the permeable crack model assumes that the crack does not perturb the electrical fields directly and that both the electric potential and the normal component of electric displacement are continuous across the crack faces. In this sense, the crack is treated as if it remains closed in its undeformed configuration. Finally, the "exact" electrical boundary conditions originally proposed by Hao and Shen (1994) attempt to account for the fact that the permittivity of the crack gap is in fact finite and the crack can in fact be open. Hence, the electric field in the gap is approximated as the potential drop divided by the crack opening displacement and the electric displacement in the gap is just this electric field multiplied by the dielectric permittivity of the gap material. Each of the model types described assumes that the crack faces are traction free.

Simply by considering the discussion of these three models for the boundary conditions it is clear that the "exact" electrical boundary conditions are the most physically realistic. However, recently McMeeking (2004) investigated the energy release rates for a Griffith crack using this type of crack face boundary condition and found that there exists a discrepancy between the energy release rate as computed from energy changes of the entire system, i.e. the total energy release rate, and the crack tip energy release rate. Here it is worthwhile to discuss why such a discrepancy between the total and crack tip energy release rates is problematic for the system under consideration. First, all parts of the system are assumed to be conservative, i.e. there is no dissipation except for energy flux through the crack tip. Second, the crack tip is assumed to be able to sustain a singularity in the electromechanical fields and no model is used to represent the material separation process ahead of the crack. This is in contrast to growing cracks in dissipative materials or models for material separation like the Dugdale–Barenblatt model, wherein distinct far field or applied energy release rates (not equivalent to the total energy release rate) and local crack tip energy release rates are commonly identified. In an entirely conservative system the crack tip energy release rate can be computed either from a crack closure integral or from the J-integral with a small contour near the crack tip. Such a calculation yields the amount of energy "flowing" into the crack tip for an infinitesimal amount of crack advance. Next, the total energy release rate for a conservative system is calculated by assembling the stored energy of all parts of the material system, including any parts of the crack gap that can store energy, and the potential energy of the loading system and then differentiating this energy with respect to crack length (care must be taken in the interpretation of this result when there are two crack tips). Note again that the definition of the total energy release rate used here for conservative systems is *not* the same as the far field or applied energy release rate that is used when dissipation is modeled directly during crack growth. Therefore, since all sources of energy are accounted for when computing the total energy release rate, including the energy entering the crack gap, and since there are no other dissipative sinks for energy to flow to aside from the crack tip, the total energy release rate must be equal to the energy release rate computed at the crack tip within a physically consistent model for the system. Hence, a discrepancy between the total and crack tip energy release rates in a conservative system is unsettling and casts doubt on the validity of the "exact" electrical boundary conditions.

In this work energetically consistent boundary conditions will be derived with an electrical component that is identical to the "exact" electrical boundary condition plus an additional closing traction. The model Griffith crack system will be used to demonstrate that these boundary conditions make the electrical enthalpy of the piezoelectric solid/crack void system stationary and that the total energy release rate is in fact equivalent to the crack tip energy release rate.

2. Theoretical foundations

Consider the electromechanically active solid depicted in Fig. 1. The equations governing a small deformation, quasi-static, isothermal boundary value problem for the solid are as follows. Mechanical equilibrium governs the stress distributions as

$$\sigma_{ji,j} + b_i = 0 \quad \text{and} \quad \sigma_{ji} = \sigma_{ij} \quad \text{in } V \tag{2.1}$$

$$(\sigma_{ji}^{+} - \sigma_{ji}^{-})n_j = t_i \quad \text{on } S \tag{2.2}$$

Here σ_{ij} represents the Cartesian components of the Cauchy stress tensor, b_i the components of the body force per unit volume, t_i the components of the surface traction, and n_i the components of the unit normal to the surface pointing from the + side to the − side as illustrated in Fig. 1. In all cases summation is assumed from 1 to 3 over repeated indices, and the notation $_{,j}$ represents partial differentiation with respect to x_j, i.e. $_{,j} \equiv \partial/\partial x_j$. Note that Eq. (2.1) neglects any electrical "Maxwell stress" terms that could potentially give rise to a body force due to electrical effects.

Next, the components of the infinitesimal strain tensor ε_{ij} are related to the components of the material displacement u_i as

$$\varepsilon_{ij} = \frac{1}{2}(u_{i,j} + u_{j,i}) \tag{2.3}$$

Under quasi-static conditions, the electrical field variables are governed by Gauss' law and Maxwell's law that states that the electrical field must be irrotational.

$$D_{i,i} = q \quad \text{in } V \tag{2.4}$$

$$(D_i^{+} - D_i^{-})n_i = -\omega \quad \text{on } S \tag{2.5}$$

$$E_i = -\phi_{,i} \tag{2.6}$$

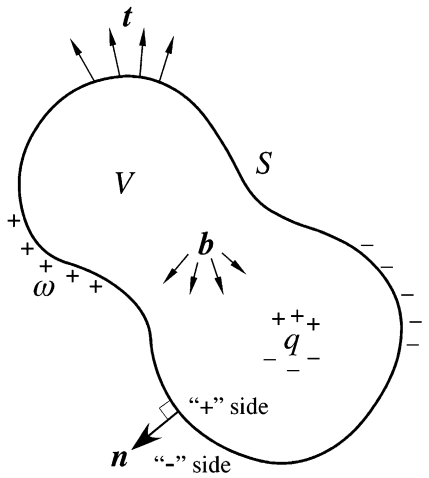

Fig. 1. An electromechanically active solid of volume V bounded by the surface S. The "+" and "−" sides of the surface are related to the direction of the unit normal to the surface $\boldsymbol{n}$ as shown. The applied electromechanical loadings include specified mechanical surface tractions $\boldsymbol{t}$ and body forces $\boldsymbol{b}$, and electrical surface free charge densities ω and body free charge densities q.

Here, D_i are the components of the electric displacement, q is a body charge per unit volume, ω is a surface charge per unit area, E_i are the components of the electric field, and ϕ is the electric potential.

To complete the set of equations the constitutive law for the material is required. In this work only conservative materials will be considered. Hence, an electrical enthalpy density h, Li and Ting (1957), can be defined such that

$$h = \tilde{u} - E_i D_i \tag{2.7}$$

where $\tilde{u}$ is the internal energy density of the material. For conservative materials

$$\mathrm{d}\tilde{u} = \sigma_{ij}\mathrm{d}\varepsilon_{ij} + E_i \mathrm{d}D_i \tag{2.8}$$

Then, Eq. (2.8) implies that

$$\mathrm{d}h = \sigma_{ij}\mathrm{d}\varepsilon_{ij} - D_i \mathrm{d}E_i \tag{2.9}$$

Ultimately, the stresses and electric displacements can be derived from h as

$$\sigma_{ij} = \frac{\partial h}{\partial \varepsilon_{ij}} \tag{2.10}$$

and

$$D_i = -\frac{\partial h}{\partial E_i} \tag{2.11}$$

Eqs. (2.1)–(2.11) represent the strong form of the governing equations for the electromechanical fields. The weak form of the equations states that the solution to the boundary value problem renders the functional $\Omega(\mathbf{u}, \phi)$ stationary, Suo et al. (1992), i.e.

$$\delta\Omega = 0 \tag{2.12}$$

where

$$\Omega(\mathbf{u}, \phi) = \int_V h \,\mathrm{d}V - \int_V b_i u_i \,\mathrm{d}V + \int_V q\phi \,\mathrm{d}V - \int_{S_\mathrm{t}} t_i u_i \,\mathrm{d}S + \int_{S_\omega} \omega\phi \,\mathrm{d}S \tag{2.13}$$

Here the total surface S consists of a region where tractions are applied S_t, displacements are prescribed S_u, free charges are applied S_ω, and electric potential is prescribed S_ϕ, with $S_u \cap S_\mathrm{t} = 0$, $S_\phi \cap S_\omega = 0$ and $S_u \cup S_\mathrm{t} = S_\phi \cup S_\omega = S$. When carrying out the operations in Eq. (2.12) the variations of the applied body forces in V, applied free charge density in V, applied tractions on S_t, and applied free surface charge density on S_ω are zero. Also, the variational strains and electric fields required to evaluate δh must be compatible with δu_i and $\delta\phi$ according to Eqs. (2.3) and (2.6). Finally, δu_i must be zero on S_u and $\delta\phi$ must be zero on S_ϕ. In the following section a model for the cracked solid and crack gap system will be described, then (2.12) and (2.13) will be applied to derive energetically consistent boundary conditions for the crack faces.

3. Energetically consistent boundary conditions

When modeling cracks in electromechanically active materials with small deformation kinematics, a dilemma arises when attempting to specify the boundary conditions on the crack faces. If a crack is modeled as an ideal slit, then in the undeformed configuration of the body the crack faces are closed and the crack should not be able to perturb the electrical fields. These considerations lead to the electrically permeable boundary conditions which assume that the crack is traction free but the jumps in both the electric potential and normal component of electric displacement across the crack are zero, Parton (1976). On the

other hand, under conditions when crack propagation is likely to occur, it is clear that the crack will actually be open and hence the medium within the crack gap will be able to support electric field and electric displacement. An approximate model for this situation results from the realization that the permittivity of free space or air is usually much lower than most solids of interest. As such, this discrepancy in permittivity is taken to the extreme and it is assumed that the permittivity of the crack gap is zero and hence the normal component of the electric displacement on the crack faces must be zero, Deeg (1980), Pak (1992), Sosa (1992), Suo et al. (1992) and many others. Lastly, another approximate model proposed by Hao and Shen (1994) treats the crack gap as a finite permittivity gap such that the electrical boundary conditions on the crack faces satisfy,

$$D_{\mathrm{c}} = \kappa_0 E_{\mathrm{c}} = -\kappa_0 \frac{\Delta\phi}{\Delta u_n} \tag{3.1}$$

Here D_{c} is the normal component of electric displacement supported by the crack gap, E_{c} is the electric field in the crack gap, κ_0 is the linear dielectric permittivity of the gap and this is usually identified with the permittivity of free space 8.854×10^{-12} C/V m. Then the electric field in the gap is computed from the solution for the solid and is given by the drop in electric potential $-\Delta\phi$ across the crack divided by the crack opening displacement Δu_n, where the subscript n represents the component of displacement normal to the crack. Note that it is assumed that any electric field components within the gap parallel to the crack can be neglected in comparison to the electric field normal to the crack. These electrical boundary conditions along with traction free mechanical boundary conditions have been investigated by numerous authors including Hao and Shen (1994), Sosa and Khutoryansky (1996), McMeeking (1999), Xu and Rajapakse (2001), Gruebner et al. (2003), and McMeeking (2004) among others. Recently, McMeeking (2004) has shown that this combination of electrical and mechanical boundary conditions leads to a discrepancy between the total and crack tip energy release rates for a Griffith crack configuration. The boundary conditions proposed here will repair this discrepancy.

In order to determine the consistent boundary conditions for a crack gap that is able to support electrical fields the following procedure is performed. First, the variation of the total electrical enthalpy of a combined cracked solid and crack gap system is derived. Then, a second system is proposed with the crack gap removed, and in its place tractions and surface charge densities are applied to the crack surfaces. In order for these two systems to be equivalent, the variations of the total electrical enthalpy of these systems must be identical for arbitrary variations of the crack face displacement and electric potential. Applying these identities will allow for the identification of effective tractions and surface charge densities that are applied by the crack gap medium to the cracked body.

Consider a cracked body subjected to some set of applied electrical and mechanical loads. The crack need not be straight or planar and can be represented as the surface S_{c} contained within the solid. The total electrical enthalpy of the solid-crack system can then be written as

$$\Omega(\mathbf{u}, \phi) = \int_V h \,\mathrm{d}V + \int_{S_{\mathrm{c}}} h_{\mathrm{c}} \Delta u_n \,\mathrm{d}S - \int_V b_i u_i \,\mathrm{d}V + \int_V q\phi \,\mathrm{d}V - \int_{S_{\mathrm{t}}} t_i u_i \,\mathrm{d}S + \int_{S_\omega} \omega\phi \,\mathrm{d}S \tag{3.2}$$

Here the second term on the right hand side has been included to account for the electrical enthalpy of the crack gap that has an electrical enthalpy density of h_{c}. Note that it is assumed that the separation of the crack surfaces is small such that the volume of the crack gap is given by $V_{\mathrm{c}} = \Delta u_n S_{\mathrm{c}}$. In essence, the evaluation of this second term is carried out in the deformed configuration of the body while the remaining terms are evaluated in the undeformed configuration. Herein lies a fundamental inconsistency with this model that can only be properly removed with a more general large deformation analysis. However, the assumptions associated with Eq. (3.2) are entirely consistent with the boundary conditions proposed in (3.1) that appear extensively in the literature.

It is assumed that the electrical enthalpy density of the crack gap h_c only depends on the electric field in the crack gap, i.e. $h_c = h_c(E_c)$. It will also be assumed that the crack gap is isotropic such that the electric displacement in the crack gap is aligned with the electric field in the gap. Such assumptions are consistent with free space or an unpressurized fluid filling the gap. Then the electric displacement within the crack gap is given as

$$D_c = -\frac{dh_c}{dE_c} \tag{3.3}$$

Again, it is important to note that both E_c and D_c are assumed to be normal to the crack plane at any given point on the crack surface. Next consider the variation of the total electrical enthalpy.

$$\begin{aligned}\delta\Omega = &\int_V \left(\frac{\partial h}{\partial \varepsilon_{ij}}\delta\varepsilon_{ij} + \frac{\partial h}{\partial E_i}\delta E_i\right) dV + \int_{S_c}\left(\Delta u_n \frac{dh_c}{dE_c}\delta E_c + h_c \delta \Delta u_n\right) dS - \int_V b_i \delta u_i \, dV + \int_V q\delta\phi \, dV \\ &- \int_{S_t} t_i \delta u_i \, dS + \int_{S_\omega} \omega \delta\phi \, dS\end{aligned} \tag{3.4}$$

Using the fact that

$$E_c = -\frac{\Delta\phi}{\Delta u_n} \tag{3.5}$$

δE_c can be shown to be

$$\delta E_c = -\frac{1}{\Delta u_n}\delta\Delta\phi + \frac{\Delta\phi}{(\Delta u_n)^2}\delta\Delta u_n \tag{3.6}$$

Then, by applying (3.3) and (3.5) the second term of Eq. (3.4) can be written as

$$\int_{S_c}\left(\Delta u_n \frac{dh_c}{dE_c}\delta E_c + h_c \delta\Delta u_n\right) dS = \int_{S_c} [D_c \delta\Delta\phi + (h_c + D_c E_c)\delta\Delta u_n] \, dS \tag{3.7}$$

Recall that this term represents the variation of the contribution to the total electrical enthalpy from the crack. This term consists of an electrical contribution associated with the electric field acting through the crack gap *plus* a mechanical contribution arising from the fact that the stored electrical energy within the crack gap increases as the volume of the gap increases. Hence, there is an increase in energy of the system associated with increasing crack opening displacement, and the work conjugate force for this configurational change is equivalent to the internal energy density of the crack gap, i.e. $h_c + E_c D_c = \tilde{u}_c$. For reasons that will become clear, this work conjugate force will be renamed σ_c or the effective stress within the crack gap. Such stresses that occur due to displacements and electrical effects are common in more general studies on large deformation behavior of electrically active materials and are referred to as Maxwell stresses.

Next, apply the facts that $\Delta u_n = -u_i^+ n_i^+ - u_i^- n_i^-$ where n_i^+ and n_i^- are the unit normal along the top and bottom crack faces respectively pointing out from the solid material as illustrated in Fig. 2, and $n_i^+ = -n_i^-$. Then, expanding S_c into top S_c^+ and bottom S_c^- surfaces, Eq. (3.4) can be rewritten as

$$\begin{aligned}\delta\Omega = &\int_V (\sigma_{ij}\delta\varepsilon_{ij} - D_i \delta E_i) \, dV + \int_{S_c^+} D_c \delta\phi^+ \, dS + \int_{S_c^-} (-D_c)\delta\phi^- \, dS - \int_{S_c^+} (\sigma_c n_i^+)\delta u_i^+ \, dS \\ &- \int_{S_c^-} (\sigma_c n_i^-)\delta u_i^- \, dS - \int_V b_i \delta u_i \, dV + \int_V q\delta\phi \, dV - \int_{S_t} t_i \delta u_i \, dS + \int_{S_\omega} \omega\delta\phi \, dS\end{aligned} \tag{3.8}$$

Eq. (3.8) represents the variation of the total electric enthalpy for a cracked solid/crack gap system. Next consider the total electrical enthalpy $\overline{\Omega}$ of only the cracked solid, but now with surface tractions t_i^+ and t_i^- and surface charge densities ω^+ and ω^- applied to the crack surfaces S_c^+ and S_c^- respectively. The purpose is

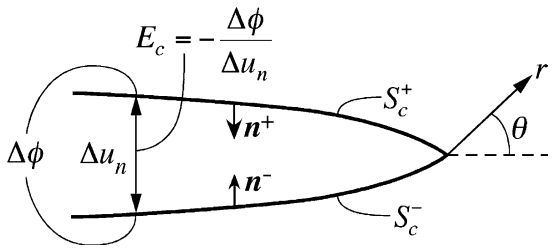

Fig. 2. Conventions for top and bottom crack surfaces S_c^+ and S_c^-, the crack opening displacement Δu_n, the potential drop $\Delta\phi = \phi^+ - \phi^-$, and the electric field within the crack gap E_c. Also shown is the polar coordinate system attached to the crack tip which will be used for the definition of the intensity factors K_I and K_D for crack problems in linear piezoelectric solids.

to determine these tractions and charges such that the field solutions in the cracked solid in this second system are identical to those in the first. The total electrical enthalpy of the cracked solid with these crack face tractions and charges is

$$\overline{\Omega}(\mathbf{u},\phi) = \int_V h\,\mathrm{d}V + \int_{S_c^+} \omega^+\phi^+\,\mathrm{d}S + \int_{S_c^-} \omega^-\phi^-\,\mathrm{d}S - \int_{S_c^+} t_i^+ u_i^+\,\mathrm{d}S - \int_{S_c^-} t_i^- u_i^-\,\mathrm{d}S - \int_V b_i u_i\,\mathrm{d}V + \int_V q\phi\,\mathrm{d}V - \int_{S_t} t_i u_i\,\mathrm{d}S + \int_{S_\omega} \omega\phi\,\mathrm{d}S \tag{3.9}$$

Then, the variation of the total electrical enthalpy for this system is

$$\delta\overline{\Omega} = \int_V (\sigma_{ij}\delta\varepsilon_{ij} - D_i\delta E_i)\,\mathrm{d}V + \int_{S_c^+} \omega^+\delta\phi^+\,\mathrm{d}S + \int_{S_c^-} \omega^-\delta\phi^-\,\mathrm{d}S - \int_{S_c^+} t_i^+\delta u_i^+\,\mathrm{d}S - \int_{S_c^-} t_i^-\delta u_i^-\,\mathrm{d}S - \int_V b_i\delta u_i\,\mathrm{d}V + \int_V q\delta\phi\,\mathrm{d}V - \int_{S_t} t_i\delta u_i\,\mathrm{d}S + \int_{S_\omega} \omega\delta\phi\,\mathrm{d}S \tag{3.10}$$

The strategy is now to choose the crack face surface tractions and charges, such that the displacement and electrical potential fields that satisfy $\delta\Omega = 0$ and $\delta\overline{\Omega} = 0$ are identical for both systems. This is accomplished by setting $\delta\overline{\Omega} = \delta\Omega$ for arbitrary variations of the displacement and electrical potential fields. Hence, from Eqs. (3.8) and (3.10) the boundary conditions for the crack surfaces are obtained. Specifically, the results for the energetically consistent crack face boundary conditions for a crack gap with an electrical enthalpy density given by $h_c(E_c)$ with E_c given by Eq. (3.5) are

$$\omega^+ = -D_i n_i^+ = D_c = -\frac{\mathrm{d}h_c}{\mathrm{d}E_c} \quad \text{on } S_c^+ \tag{3.11}$$

$$\omega^- = -D_i n_i^- = -D_c = \frac{\mathrm{d}h_c}{\mathrm{d}E_c} \quad \text{on } S_c^- \tag{3.12}$$

$$t_i^+ = \sigma_{ji} n_j^+ = \sigma_c n_i^+ = (h_c + E_c D_c) n_i^+ \quad \text{on } S_c^+ \tag{3.13}$$

$$t_i^- = \sigma_{ji} n_j^- = \sigma_c n_i^- = (h_c + E_c D_c) n_i^- \quad \text{on } S_c^- \tag{3.14}$$

Eqs. (3.11)–(3.14) represent the primary result for this section of the paper. It is very important to note that these boundary conditions depend on the solution for the fields in the solid in a *non-linear* fashion due to the definition of the electric field in the crack given by Eq. (3.5). In the following, more specific forms for

these boundary conditions will be given for the special cases of perfect linear dielectric crack gap behavior and an idealized model for electrical discharge within the crack gap.

3.1. The linear dielectric crack gap

Consider a crack gap with linear dielectric behavior described by Eq. (3.1) that has been studied by numerous authors. Specifically, the electric field versus electric displacement behavior of the gap is assumed to be

$$D_{\mathrm{c}} = \kappa_0 E_{\mathrm{c}} \tag{3.15}$$

Here κ_0 is the dielectric constant of the material filling the crack gap and in most situations is identified as the dielectric permittivity of free space. Then, the electrical enthalpy density of the crack gap for this case is

$$h_{\mathrm{c}} = -\frac{1}{2}\kappa_0 E_{\mathrm{c}}^2 \tag{3.16}$$

Finally, the crack boundary conditions can be stated as

$$D_n^+ = D_n^- = -\kappa_0 \frac{\phi^+ - \phi^-}{u_n^+ - u_n^-} \quad \text{on } S_{\mathrm{c}}^+ \text{ and } S_{\mathrm{c}}^- \tag{3.17}$$

and

$$\sigma_{nn}^+ = \sigma_{nn}^- = \frac{1}{2}\kappa_0 \left(\frac{\phi^+ - \phi^-}{u_n^+ - u_n^-} \right)^2 \quad \text{on } S_{\mathrm{c}}^+ \text{ and } S_{\mathrm{c}}^- \tag{3.18}$$

Here a convention is defined on the crack faces such that the subscript n represents the component normal to the crack surfaces with the positive direction associated with the lower crack face normal. Specifically, $D_n^+ = D_i^+ n_i^-$, $D_n^- = D_i^- n_i^-$, $u_n^+ = u_i^+ n_i^-$, $u_n^- = u_i^- n_i^-$, $\sigma_{nn}^+ = \sigma_{ji}^+ n_j^- n_i^-$ and $\sigma_{nn}^- = \sigma_{ji}^- n_j^- n_i^-$ (no summation over n). Note that for the standard crack configuration with the crack lying along the x_1-axis and perpendicular to the x_2-axis, the subscript n in Eqs. (3.17) and (3.18) can be replaced by a numeral 2. Also note that the electric displacements and stresses denoted in these equations are those quantities in the solid at the crack surface. Finally, Eq. (3.17) is the so-called "exact" boundary condition that has received considerable study in the literature. However, aside from the work of Landis and McMeeking (2000), the non-zero traction component of these boundary conditions has yet to be recognized or studied.

3.2. The non-linear electrically discharging crack gap

For materials that have dielectric constants much higher than that of the gap, the electric fields in the crack gap can be magnified considerably over those in the solid. Under such circumstances it is likely that the gap material will break down electrically by the mechanism of corona discharges. Here, a very simple phenomenological model is proposed for such electrical discharge. It will be assumed that the crack gap will behave in a linear dielectric fashion up to some critical electric field level for discharge E_{d}. At this point the electric displacement in the gap will be $D_{\mathrm{c}} = \kappa_0 E_{\mathrm{d}}$. It will be assumed that the crack gap cannot support electric fields larger than E_{d}, but that charge can be transferred between the crack faces such that the effective electric displacement of the crack gap can increase without bound. In effect, at the critical level of the electric field the gap becomes conducting. However, in this work we are interested in quasi-static behavior and hence the conductance of the gap is not the issue, but the amount of charge transferred during the discharge is. This model for discharge in the crack gap is analogous to the critical electric field model for electrical breakdown in solids used by Zhang and Gao (2004).

For this simple model for discharge, the electric displacement in the crack gap takes on the mathematical form,

$$D_c = \kappa_0 E_c \quad \text{if } |D_c| \leqslant \kappa_0 E_d \tag{3.19}$$

$$D_c = \text{sgn}(\omega_d)\kappa_0 E_d + \omega_d \quad \text{and} \quad E_c = \text{sgn}(\omega_d)E_d \quad \text{if } |D_c| \geqslant \kappa_0 E_d \tag{3.20}$$

Here ω_d represents the amount of charge per unit area transferred between the crack faces. Such a transfer of charge is an irreversible process, but for the purposes of this work will be modeled as reversible. The reversible and irreversible cases are indistinguishable from one another as long as no electrical unloading of the crack gap occurs. Then, the electrical enthalpy density of the crack gap can be given as

$$h_c = -\frac{1}{2}\kappa_0 E_c^2 \quad \text{if } |D_c| \leqslant \kappa_0 E_d \tag{3.21}$$

$$h_c = -\frac{1}{2}\kappa_0 E_d^2 \quad \text{if } |D_c| \geqslant \kappa_0 E_d \tag{3.22}$$

Then if $|D_c| \leqslant \kappa_0 E_d$ the boundary conditions along the crack faces can be given as

$$D_n^+ = D_n^- = -\kappa_0 \frac{\phi^+ - \phi^-}{u_n^+ - u_n^-} \quad \text{on } S_c^+ \text{ and } S_c^- \tag{3.23}$$

and

$$\sigma_{nn}^+ = \sigma_{nn}^- = \frac{1}{2}\kappa_0 \left(\frac{\phi^+ - \phi^-}{u_n^+ - u_n^-} \right)^2 \quad \text{on } S_c^+ \text{ and } S_c^- \tag{3.24}$$

If $|D_c| \geqslant \kappa_0 E_d$ the boundary conditions are

$$-\frac{\phi^+ - \phi^-}{u_n^+ - u_n^-} = \text{sgn}(D_c)E_d \quad \text{on } S_c^+ \text{ and } S_c^- \tag{3.25}$$

$$D_n^+ = D_n^- = \kappa_0 \text{sgn}(D_c)E_d + \omega_d \quad \text{on } S_c^+ \text{ and } S_c^- \tag{3.26}$$

and

$$\sigma_{nn}^+ = \sigma_{nn}^- = E_d|D_c| - \frac{1}{2}\kappa_0 E_d^2 = E_d|\omega_d| + \frac{1}{2}\kappa_0 E_d^2 \quad \text{on } S_c^+ \text{ and } S_c^- \tag{3.27}$$

These boundary conditions will be used to analyze a Griffith crack in a linear piezoelectric solid in Section 5 of this paper.

4. Evaluation of the crack tip energy release rate G_{tip} using the J-integral

Consider a straight through-thickness crack in a solid parallel to the x_1 direction as drawn in Fig. 3. The J-integral J_Γ for a contour Γ beginning on the bottom crack face, traveling around the crack tip and ending on the top crack face is defined as

$$J_\Gamma = \int_\Gamma (hn_1 - \sigma_{ji}n_j u_{i,1} + D_i n_i E_1)\,d\Gamma \tag{4.1}$$

Here n_i are the components of the unit vector normal to the contour Γ and pointing to the right. It should be noted that there exist three other forms of the J-integral for electromechanical fracture, however the

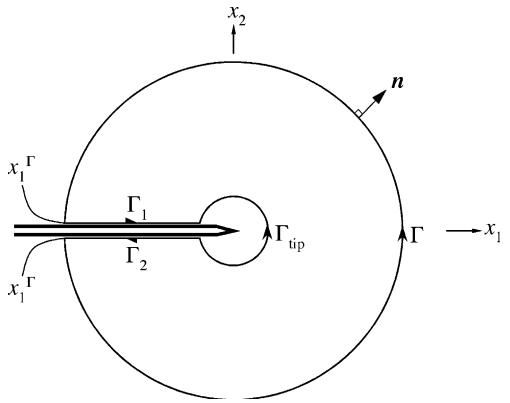

Fig. 3. The contours used for analyzing the relationship between the J-integral and the energy release rate. The crack is parallel to the x_1 direction and the outer contour Γ intersects the top and bottom crack faces at the same x_1 position x_1^Γ.

form of Eq. (4.1) is the most useful for finite element computations and will be the only one treated here. Note that J_Γ is equal to zero for a closed contour in a regular region of material containing no cracks or other singularities. Furthermore, J_Γ yields the amount of energy entering the contour per unit of virtual advance of the contour and crack in the x_1 direction. For situations where the constitutive behavior of the solid is reversible and the region between the crack faces cannot remove energy from the system, the energy entering into the contour must be balanced by the energy flowing out through the crack tip. Therefore, under such conditions, J_Γ is equal to the crack tip energy release rate G_{tip} and is independent of the path Γ. These path-independent conditions arise when the crack faces are traction free and the normal component of electric displacement vanishes. However, for the crack model described in Section 3 the region between the crack faces can store energy and hence the energy entering the contour Γ is balanced by the energy flowing out through both the crack tip and the crack faces. Under these conditions J_Γ is not equal to G_{tip} and J_Γ is not path-independent. However, a simple relationship between J_Γ and G_{tip} can still be obtained.

Consider the closed contour illustrated in Fig. 3. The contour Γ_{tip} will be shrunken onto the crack tip such that $J_{\text{tip}} = G_{\text{tip}}$. For the following derivation it will be required that the outer contour intersects the top and bottom crack faces at the same x_1 position and this position will be called x_1^Γ. Then, the facts that the J-integral is zero around the closed contour and the closed contour must traverse Γ_{tip} in the clockwise direction imply that

$$J_\Gamma + J_1 + J_2 - J_{\text{tip}} = 0. \tag{4.2}$$

Eq. (4.2) can be expanded into

$$G_{\text{tip}} = J_\Gamma + \int_{x_1^\Gamma}^{0} (\sigma_{2i}^+ u_{i,1}^+ + D_2^+ \phi_{,1}^+)\,\mathrm{d}x_1 + \int_0^{x_1^\Gamma} (\sigma_{2i}^- u_{i,1}^- + D_2^- \phi_{,1}^-)\,\mathrm{d}x_1 \tag{4.3}$$

Next applying the boundary conditions given by Eqs. (3.11)–(3.14), using $\Delta u_2 = u_2^+ - u_2^-$ and $\Delta\phi = \phi^+ - \phi^-$, and interchanging the limits of integration of the second term yields

$$G_{\text{tip}} = J_\Gamma + \int_{x_1}^{0} [(h_{\text{c}} + E_{\text{c}} D_{\text{c}})\Delta u_{2,1} + D_{\text{c}} \Delta\phi_{,1}]\,\mathrm{d}x_1 \tag{4.4}$$

The integrand of the second term of Eq. (4.4) can be manipulated as follows

$$\begin{aligned}(h_c + E_c D_c)\Delta u_{2,1} + D_c \Delta\phi_{,1} &= [(h_c + E_c D_c)\Delta u_2 + D_c \Delta\phi]_{,1} - (h_{c,1} + E_{c,1} D_c + E_c D_{c,1})\Delta u_2 - D_{c,1}\Delta\phi \\ &= \left[\left(h_c - \frac{\Delta\phi}{\Delta u_2} D_c\right)\Delta u_2 + D_c \Delta\phi\right]_{,1} - \left(h_{c,1} + E_{c,1} D_c - \frac{\Delta\phi}{\Delta u_2} D_{c,1}\right)\Delta u_2 - D_{c,1}\Delta\phi \\ &= (h_c \Delta u_2)_{,1} - (h_{c,1} + E_{c,1} D_c)\Delta u_2 = (h_c \Delta u_2)_{,1} - \left(\frac{\mathrm{d}h_c}{\mathrm{d}E_c} E_{c,1} + E_{c,1} D_c\right)\Delta u_2 \\ &= (h_c \Delta u_2)_{,1} - (-D_c E_{c,1} + E_{c,1} D_c)\Delta u_2 = (h_c \Delta u_2)_{,1} \end{aligned} \tag{4.5}$$

Finally, the fact that the jumps in displacement and electric potential are zero at the crack tip and assuming that the electrical enthalpy density at the tip is finite allows for the final result

$$G_{\mathrm{tip}} = J_\Gamma - h_c(x_1^\Gamma)\Delta u_2(x_1^\Gamma) \tag{4.6}$$

Hence, a full integral along the crack faces is not required to determine G_{tip}. The crack tip energy release rate G_{tip} can be obtained by computing a single J-contour integration and then subtracting the electrical enthalpy density of the crack gap times the crack opening displacement evaluated at the intersection of the J-contour with the crack surfaces. It is important to note that J_Γ is dependent on the path Γ and is *not* the total energy release rate, and in general cannot be interpreted as the applied energy release rate either.

5. The Griffith crack in a poled linear piezoelectric solid

In this section the energetically consistent boundary conditions described in Section 3 will be applied to the Griffith crack in a poled linear piezoelectric solid. For simplicity the material will be poled perpendicular to the crack and only Mode I and D loadings will be applied to the sample. The extension to include Mode II and III loadings is straightforward, but only acts to complicate the governing equations. First, the solution for the fundamental Griffith crack problem with uniform charge and traction acting on the crack surfaces will be reviewed and important features of the solution will be outlined. Then, this solution will be applied to analyze the Griffith crack problem with applied loading in the far field and with the crack gap able to store energy. It will be shown again that the boundary conditions derived in Section 3 prevail and that the total energy release rate computed from energy variations of the entire system is equivalent to the crack tip energy release rate with these boundary conditions. Finally, specific cases will be solved and compared to ascertain the effects of the energetically consistent boundary conditions and especially the effects of electrical discharge within the crack.

5.1. The fundamental Griffith crack solution

Here the solution for a Griffith crack of length $2a$ in a non-polar linear piezoelectric solid loaded by a uniform opening traction σ^* and a uniform charge distribution D^* on the crack faces as shown in Fig. 4 will be outlined. Note that here the crack gap does not support any stress, electric field or electric displacement. This solution has appeared in the literature many times and the details of its derivation will not be repeated here. Instead, only the features of the solution that will be required for the subsequent analyses will be given.

First the constitutive behavior of the solid material is given as

$$\sigma_{ij} = c^E_{ijkl}\varepsilon_{kl} - e_{kij}E_k \tag{5.1}$$

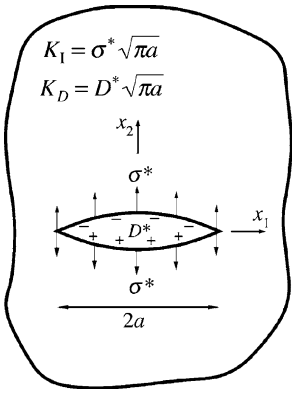

Fig. 4. A schematic of the Griffith crack problem with electromechanical loading applied only to the crack faces. Features of the solution for this problem in a linear piezoelectric solid with no energy stored in the crack gap are given in Eqs. (5.4)–(5.13). The intensity factors for this problem, K_I and K_D, are also listed.

$$D_i = e_{ikl}\varepsilon_{kl} + \kappa^{\varepsilon}_{ij}E_j + P^r_i \tag{5.2}$$

Here c^E_{ijkl}, e_{kij} and $\kappa^{\varepsilon}_{ij}$ are the Cartesian components of the elastic stiffness at constant electric field, piezoelectricity, and dielectric permittivity at constant strain tensors. The components of the remanent polarization are given as P^r_i. For the problem depicted in Fig. 4 the remanent polarization is zero, $P^r_i = 0$, however the remanent polarization will be non-zero in later sections and analyses. Note that for ferroelectric materials, remanent polarization is usually accompanied by remanent strain. However, Eqs. (5.1) and (5.2) remain valid for such a material with homogeneous remanent strain and remanent polarization as long as the initial remanent strain state is taken as the reference datum for strains. A similar choice of reference for the electric displacements is not valid and the remanent polarization must be included in (5.2).

For the boundary value problem illustrated in Fig. 4, the stresses and electric displacements in the solid must go to zero in the far field and must satisfy the following conditions on the crack faces.

$$\sigma_{22} = -\sigma^*, \quad \sigma_{12} = 0, \quad \text{and} \quad D_2 = -D^* \quad \text{on } x_2 = 0, \ |x_1| < a \tag{5.3}$$

From the solution to this boundary value problem we will be interested in the crack opening displacement, the electric potential drop across the crack, the total electrical enthalpy of the solid and the loading system, the stress and electric displacement intensity factors and the crack tip energy release rate.

First, define the intensity factors K_I and K_D such that very close to the crack tip $\sigma_{22} \to K_I/\sqrt{2\pi r}$ and $D_2 \to K_D/\sqrt{2\pi r}$. Then the values for K_I and K_D can be obtained from the solution by analyzing the following limits,

$$K_I = \lim_{r\to 0}[\sigma_{22}(r, \theta = 0)\sqrt{2\pi r}] = \sigma^*\sqrt{\pi a} \tag{5.4}$$

$$K_D = \lim_{r\to 0}[D_2(r, \theta = 0)\sqrt{2\pi r}] = D^*\sqrt{\pi a} \tag{5.5}$$

Here r and θ represent a polar coordinate system centered on a crack tip as shown in Fig. 2. Then the crack tip energy release rate for one of the crack tips can be given in terms of the intensity factors as

$$G_{\text{tip}} = H_{11}K_{\text{I}}^2 + 2H_{12}K_{\text{I}}K_{\text{D}} + H_{22}K_{\text{D}}^2 \tag{5.6}$$

Here H_{11}, H_{12} and H_{22} are components of the Irwin matrix, and these quantities depend only on the material properties of the solid. Examples for the values of H_{11}, H_{12} and H_{22} are given in Appendix A. Next, the crack opening displacement and electric potential drop across the crack are given as

$$\Delta u_2(x_1) = u_2^+ - u_2^- = 4(H_{11}\sigma^* + H_{12}D^*)\sqrt{a^2 - x_1^2} \tag{5.7}$$

$$\Delta\phi(x_1) = \phi^+ - \phi^- = 4(H_{12}\sigma^* + H_{22}D^*)\sqrt{a^2 - x_1^2} \tag{5.8}$$

Lastly, the electrical enthalpy of the solid Ω_{solid} and that of the loading system Ω_{loads} can be given as

$$\Omega_{\text{solid}} = \frac{\pi}{16}(\eta_{11}\Delta u_0^2 + 2\eta_{12}\Delta u_0\Delta\phi_0 + \eta_{22}\Delta\phi_0^2) \tag{5.9}$$

$$\Omega_{\text{loads}} = -\frac{\pi}{2}a\sigma^*\Delta u_0 - \frac{\pi}{2}aD^*\Delta\phi_0 \tag{5.10}$$

Here η_{11}, η_{12} and η_{22} are the components of the inverse of the Irwin matrix and Δu_0 and $\Delta\phi_0$ are the crack opening displacement and electric potential drop across the crack at $x_1 = 0$, i.e.

$$\begin{bmatrix} \eta_{11} & \eta_{12} \\ \eta_{12} & \eta_{22} \end{bmatrix} = \begin{bmatrix} H_{11} & H_{12} \\ H_{12} & H_{22} \end{bmatrix}^{-1} \tag{5.11}$$

$$\Delta u_0 = \Delta u_2(x_1 = 0) = 4a(H_{11}\sigma^* + H_{12}D^*) \tag{5.12}$$

$$\Delta\phi_0 = \Delta\phi(x_1 = 0) = 4a(H_{12}\sigma^* + H_{22}D^*) \tag{5.13}$$

In the following subsection the results from this problem will be applied to the solution for a Griffith crack in a *polar* linear piezoelectric solid with a crack gap that is able to support electric fields.

5.2. The energetically consistent solution to the Griffith crack problem

Consider the problem illustrated in Fig. 5a. The material contains a homogeneous remanent polarization in the x_2 direction of magnitude P^r. It is important to note that practically all of the results on linear piezoelectric fracture appearing in the literature implicitly assume that either the material is non-polar or that material separation at the crack tip occurs in a very particular way. For example, if the material is poled perpendicular to the crack tip as illustrated in Fig. 5a, it is assumed that an excess of positively charged ions will separate onto the top crack face and the same excess of negative charge will separate onto the bottom crack face. Such a separation of charges can be interpreted as a surface charge density of magnitude ω_{s}, where the subscript "s" denotes "separation" or "segregation". Most researchers have tacitly assumed that ω_{s} is exactly equal to the remanent polarization P^r. Here, ω_{s} is identified as the excess surface charge density due to material separation and will be allowed to take on arbitrary values. Next, the specified applied loads in the far field consist of a uniaxial tensile stress and an electric displacement in the x_2 direction of magnitudes σ and D. Note that the applied electric displacement D can be considered as consisting of two parts, i.e. $D = \Delta D + P^r$. Here ΔD represents the excess applied electric displacement over the remanent polarization and is a result of the linear piezoelectric response of the material. Finally, the crack gap is characterized by an electrical enthalpy density h_{c}.

Fig. 5b–d illustrate that this problem can be decomposed into three separate problems. Specifically, a uniformly poled material with no crack under no applied loads, plus a non-polar material with no crack subjected to uniform applied loads σ and ΔD, plus a non-polar material with a crack subjected to the

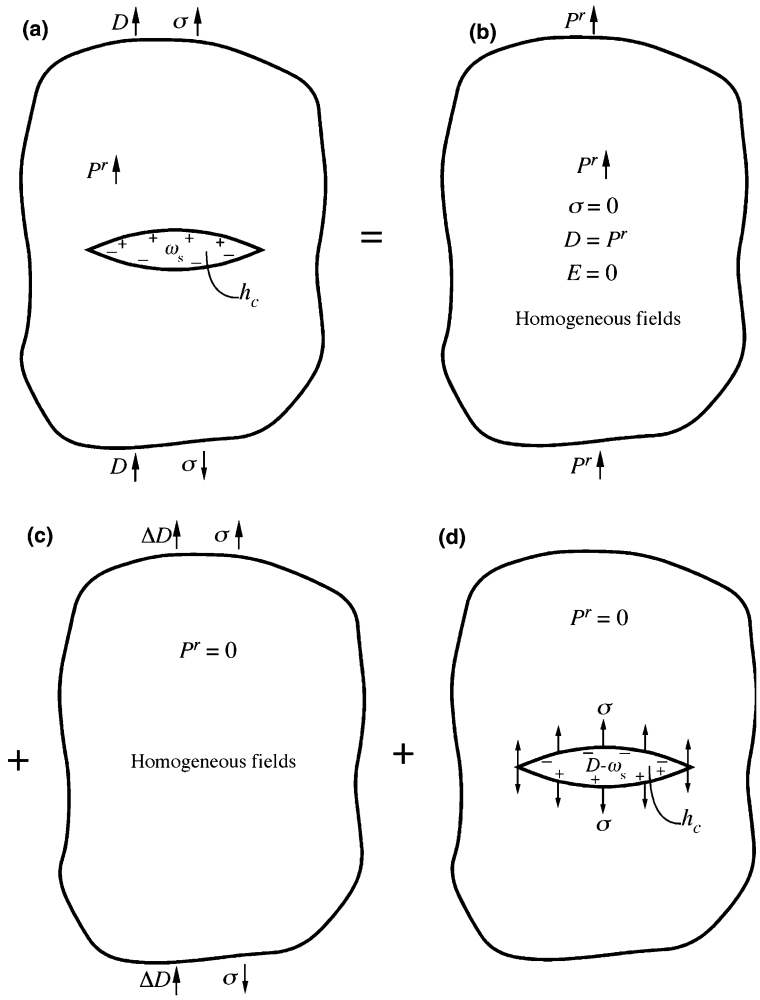

Fig. 5. The superposition scheme used to solve the Griffith crack problem with electromechanical loading in the far field and a crack gap that is able to store electrical energy. The original problem (a) allows for a linear piezoelectric and polarized solid, as well as a crack surface charge density ω_s due to charge separation/segregation during material separation. Problems (b) and (c) involve only homogeneous fields and hence the crack intensity factors and energy release rates are equivalent for problems (a) and (d).

uniform tractions and charge densities on the crack faces of magnitude σ and $D-\omega_s$. Then, since the first two parts of the decomposed problem do not contain a crack, it can be argued that the intensity factors, total energy release rate and crack tip energy release rate for the original problem (a) and the last problem (d) are identical.

We now proceed to the total electrical enthalpy for the system illustrated in Fig. 5d.

$$\begin{aligned}\Omega &= \Omega_{\text{solid}} + \Omega_{\text{loads}} + \Omega_{\text{crack}} \\ &= \frac{\pi}{16}\left(\eta_{11}\Delta u_0^2 + 2\eta_{12}\Delta u_0\Delta\phi_0 + \eta_{22}\Delta\phi_0^2\right) - \frac{\pi}{2}a\sigma\Delta u_0 - \frac{\pi}{2}a(D-\omega_s)\Delta\phi_0 + \frac{\pi}{2}a\Delta u_0 h_c\end{aligned} \tag{5.14}$$

Here it should be noted that it has been assumed that the crack will open up into an ellipse of area $A_{\text{crack}} = \pi a\Delta u_0/2$ and that the inclusion of the crack enthalpy density does not change the *shape* of either the

crack opening displacement or electric potential drop distributions. Note, however, that the inclusion of the crack enthalpy density can change the *sizes* of these distributions.

It is now assumed, in a fashion consistent with Eq. (2.12), that the solution to this problem causes the total electrical enthalpy to be stationary. Eq. (5.14) has expanded the electrical enthalpy into a function of two unknown scalar variables Δu_0 and $\Delta\phi_0$. Therefore, the following equations must be satisfied for the solution

$$\frac{\partial\Omega}{\partial\Delta u_0} = \frac{\pi}{8}(\eta_{11}\Delta u_0 + \eta_{12}\Delta\phi_0) - \frac{\pi}{2}a\sigma + \frac{\pi}{2}a\sigma_c = 0 \tag{5.15}$$

$$\frac{\partial\Omega}{\partial\Delta\phi_0} = \frac{\pi}{8}(\eta_{12}\Delta u_0 + \eta_{22}\Delta\phi_0) - \frac{\pi}{2}a(D-\omega_s) + \frac{\pi}{2}aD_c = 0 \tag{5.16}$$

Along with the definition $\sigma_c = h_c + E_cD_c$, the following relationships have been used to derive the simplified forms of Eqs. (5.15) and (5.16).

$$\frac{\partial h_c}{\partial\Delta u_0} = \frac{dh_c}{dE_c}\frac{\partial E_c}{\partial\Delta u_0} = -D_c\frac{\partial}{\partial\Delta u_0}\left(-\frac{\Delta\phi_0}{\Delta u_0}\right) = -D_c\frac{\Delta\phi_0}{\Delta u_0^2} = E_cD_c\frac{1}{\Delta u_0} \tag{5.17}$$

$$\frac{\partial h_c}{\partial\Delta\phi_0} = \frac{dh_c}{dE_c}\frac{\partial E_c}{\partial\Delta\phi_0} = -D_c\frac{\partial}{\partial\Delta\phi_0}\left(-\frac{\Delta\phi_0}{\Delta u_0}\right) = D_c\frac{1}{\Delta u_0} \tag{5.18}$$

In general, both σ_c and D_c are non-linear functions of Δu_0 and $\Delta\phi_0$ and hence Eqs. (5.15) and (5.16) represent a set of non-linear equations governing Δu_0 and $\Delta\phi_0$. Explicit solutions to these equations will be detailed later in this subsection. However, (5.15) and (5.16) can be readily manipulated to demonstrate some features of the solution.

First, by inverting the first terms of Eqs. (5.15) and (5.16), the crack opening displacement and electric potential drop across the crack can be shown to be

$$\Delta u_0 = 4a[H_{11}(\sigma-\sigma_c) + H_{12}(D-\omega_s-D_c)] \tag{5.19}$$

$$\Delta\phi_0 = 4a[H_{12}(\sigma-\sigma_c) + H_{22}(D-\omega_s-D_c)] \tag{5.20}$$

Note that this solution can be interpreted as the solution in the solid material with $\sigma^* = \sigma - \sigma_c$ and $D^* = D - \omega_s - D_c$. Hence, the intensity factors and the crack tip energy release rate are given as

$$K_I = (\sigma-\sigma_c)\sqrt{\pi a} \tag{5.21}$$

$$K_D = (D-\omega_s-D_c)\sqrt{\pi a} \tag{5.22}$$

$$G_{tip} = \pi a[H_{11}(\sigma-\sigma_c)^2 + 2H_{12}(\sigma-\sigma_c)(D-\omega_s-D_c) + H_{22}(D-\omega_s-D_c)^2] \tag{5.23}$$

Note that the intensity factors K_I and K_D depend on the features of the energetically consistent boundary conditions σ_c and D_c. Furthermore, the levels of σ_c and D_c are dependent on K_I and K_D as will be detailed later in this section. A more detailed discussion of this coupling that arises from the energetically consistent boundary conditions and its effects on the asymptotic crack tip fields in linear piezoelectric solids is included in Appendix B.

Returning to the Griffith crack problem, by adding Eq. (5.15) multiplied by Δu_0 with Eq. (5.16) multiplied by $\Delta\phi_0$, it can be shown that

$$\eta_{11}\Delta u_0^2 + 2\eta_{12}\Delta u_0\Delta\phi_0 + \eta_{22}\Delta\phi_0^2 = 4a(\sigma-\sigma_c)\Delta u_0 + 4a(D-\omega_s-D_c)\Delta\phi_0 \tag{5.24}$$

Then, implementing Eqs. (5.19), (5.20) and (5.24), the equation for the total electrical enthalpy can be manipulated as

$$\begin{aligned}\Omega &= \frac{\pi}{16}\left(\eta_{11}\Delta u_0^2 + 2\eta_{12}\Delta u_0\Delta\phi_0 + \eta_{22}\Delta\phi_0^2\right) - \frac{\pi}{2}a\sigma\Delta u_0 - \frac{\pi}{2}a(D-\omega_s)\Delta\phi_0 + \frac{\pi}{2}a\Delta u_0 h_c \\ &= \frac{\pi}{4}a[(\sigma-\sigma_c)\Delta u_0 + 4a(D-\omega_s-D_c)\Delta\phi_0] - \frac{\pi}{2}a\sigma\Delta u_0 - \frac{\pi}{2}a(D-\omega_s)\Delta\phi_0 \\ &\quad + \frac{\pi}{2}a\Delta u_0\left(h_c + E_c D_c + D_c\frac{\Delta\phi_0}{\Delta u_0}\right) \\ &= \frac{\pi}{4}a[(\sigma-\sigma_c)\Delta u_0 + 4a(D-\omega_s-D_c)\Delta\phi_0] - \frac{\pi}{2}a\sigma\Delta u_0 - \frac{\pi}{2}a(D-\omega_s)\Delta\phi_0 + \frac{\pi}{2}a\sigma_c\Delta u_0 + \frac{\pi}{2}aD_c\Delta\phi_0 \\ &= -\frac{\pi}{4}a[(\sigma-\sigma_c)\Delta u_0 + (D-\omega_s-D_c)\Delta\phi_0] \\ &= -\pi a^2[H_{11}(\sigma-\sigma_c)^2 + 2H_{12}(\sigma-\sigma_c)(D-\omega_s-D_c) + H_{22}(D-\omega_s-D_c)^2] \end{aligned} \tag{5.25}$$

Now, recognizing that the total energy release rate per unit of crack advance for one of the crack tips is given by the opposite of the derivative of the electrical enthalpy with respect to the *total* crack length $2a$, G_{total} can be shown to be

$$G_{\text{total}} = -\frac{\partial\Omega}{\partial(2a)} = \pi a[H_{11}(\sigma-\sigma_c)^2 + 2H_{12}(\sigma-\sigma_c)(D-\omega_s-D_c) + H_{22}(D-\omega_s-D_c)^2] \tag{5.26}$$

Therefore, it has now been shown that the total energy release rate is equal to the crack tip energy release rate for this system with any arbitrary form of the electrical enthalpy density for the crack medium. For the remainder of this paper both G_{tip} and G_{total} will simply be referred to as the energy release rate G when applying the energetically consistent boundary conditions. Also, note that this solution procedure applies the weak form of the governing equations and that the crack face boundary conditions derived in Section 3 were not applied directly. However, if the strong form of the equations had been applied with the crack boundary conditions of Section 3, the solution that would have been obtained would be identical to that outlined above. We now proceed to a few specific examples.

First, Eqs. (5.15) and (5.16) will be solved for the case where the electrical enthalpy density of the crack medium is given by that described in Section 3.2. Specifically, the solution to Eqs. (5.15) and (5.16) can be obtained by the following procedure. If the electric field supported by the crack gap is less than the discharge field E_d, then the crack opening displacement is governed by the following cubic equation,

$$\begin{aligned}&\eta_{11}\frac{\Delta u_0}{a}\left(\eta_{22}\frac{\Delta u_0}{a} - 4\kappa_0\right)^2 - \eta_{12}\frac{\Delta u_0}{a}\left[\eta_{12}\frac{\Delta u_0}{a} - 4(D-\omega_s)\right]\left(\eta_{22}\frac{\Delta u_0}{a} - 4\kappa_0\right) \\ &\quad + 2\kappa_0\left[\eta_{12}\frac{\Delta u_0}{a} - 4(D-\omega_s)\right]^2 - 4\sigma\left(\eta_{22}\frac{\Delta u_0}{a} - 4\kappa_0\right)^2 = 0 \quad \text{if } \left|\frac{\Delta\phi_0}{\Delta u_0}\right| \leqslant E_d \end{aligned} \tag{5.27}$$

After obtaining the relevant solution to Eq. (5.27), the potential drop across the crack is given by

$$\Delta\phi_0 = -\Delta u_0\frac{4(D-\omega_s)a - \eta_{12}\Delta u_0}{4\kappa_0 a - \eta_{22}\Delta u_0} \quad \text{if } \left|\frac{\Delta\phi_0}{\Delta u_0}\right| \leqslant E_d \tag{5.28}$$

Fig. 6 is a contour plot of the solutions for the energy release rate (total or crack tip) predicted using the energetically consistent boundary conditions assuming no electrical discharge for wide ranges of applied stress σ and effective electric displacement $D-\omega_s$. The material properties of the linear piezoelectric material are characteristic of PZT-5H and are listed in Appendix A. The results of Fig. 6 are valid for either polar or non-polar materials. However, for polar materials $D = \Delta D + P^r$. It is common to present results like those shown in Fig. 6 with the abscissa as electric field instead of $D-\omega_s$. However, such a presentation

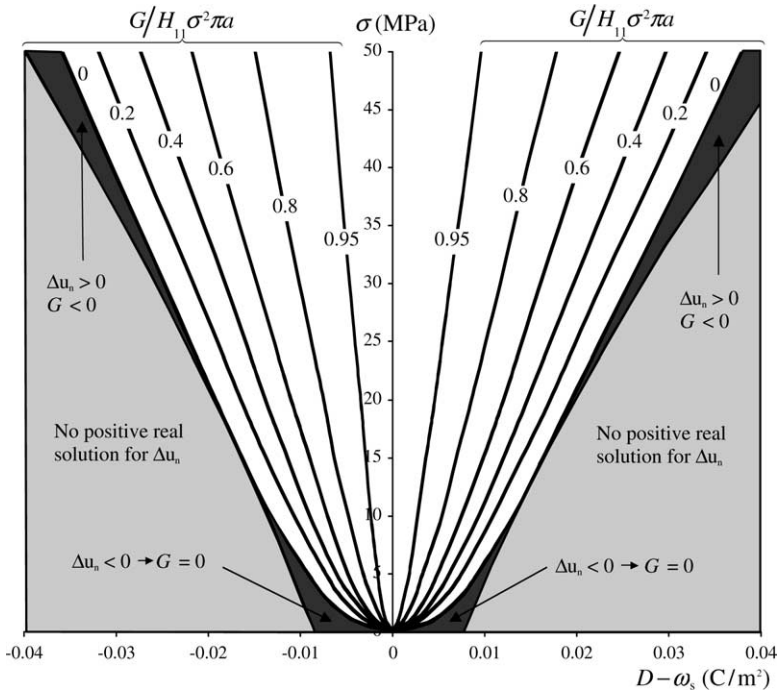

Fig. 6. A contour plot of normalized energy release rate G (total or crack tip) for a remotely loaded Griffith crack versus applied stress and applied effective electric displacement. Energetically consistent boundary conditions are applied to generate this solution. The material is linear piezoelectric with properties characteristic of PZT-5H as given in Appendix A.

would yield different results for differing levels of remanent polarization and ω_s. If the applied electric field is know instead of the electric displacement, then the electric displacement can be computed by manipulating Eqs. (5.1) and (5.2).

In order to obtain solutions for the energy release rate the solutions to Eqs. (5.27) and (5.28) for Δu_0 and $\Delta\phi_0$ must be found first. Eq. (5.27) is a cubic equation for Δu_0 and in general there will be three solutions to this equation. However, only one of these roots represents the physical solution and its characteristics are represented by shades of gray on Fig. 6. Within the white region of Fig. 6 solutions for Δu_0 are positive, real and lead to positive energy release rates. The upper dark gray sectors represent positive real solutions for Δu_0 but result in negative energy release rates. The most negative normalized level of the energy release rate in these sectors within the range shown is $G/H_{11}\sigma^2\pi a \approx -0.24$ which occurs at $\sigma \approx 46$ MPa and $D - \omega_s \approx 0.04$ C/m^2. The lower dark gray sectors represent negative real solutions for Δu_0 and hence the crack is actually closed in these regions and the energy release rate should be interpreted to be zero. Finally, within the light gray sectors the physically reasonable root to (5.27) is complex. There also exists another non-physical root that is negative within this region. In either case the interpretation is that the crack remains closed and the energy release rate is zero. The features of the solution for the energetically consistent boundary conditions differ from those for the "exact" and impermeable boundary conditions in that the regions where negative energy release rates are physically realizable are considerably smaller than those for the other models. A more detailed comparison to the impermeable and "exact" boundary condition models is included in Fig. 7.

For comparison to the impermeable and "exact" boundary conditions appearing in the literature it will be assumed that the discharge field is extremely large such that $E_d \rightarrow \infty$. The solution to the Griffith crack problem assuming impermeable boundary conditions has both $D_c = 0$ and $\sigma_c = 0$. Also, when computing

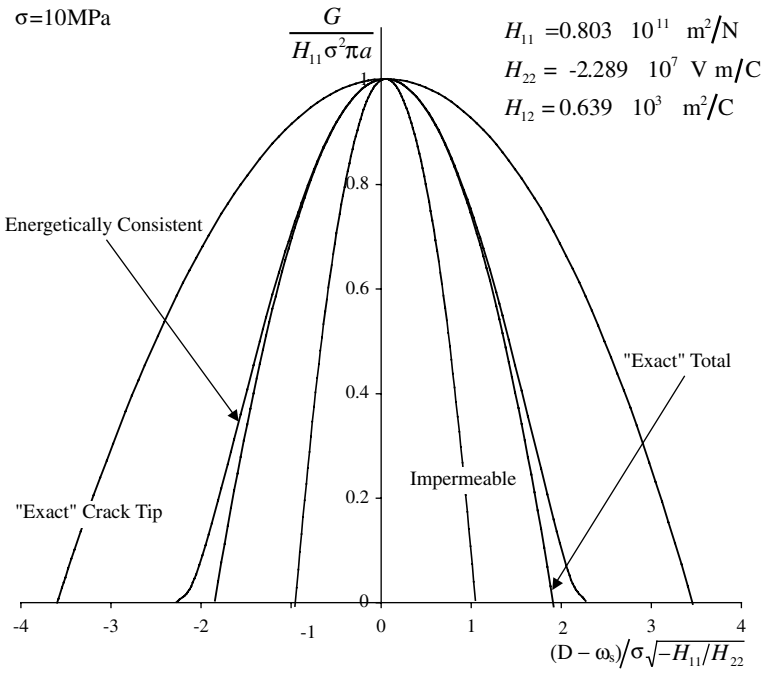

Fig. 7. Energy release rates for a Griffith crack in a linear piezoelectric solid. The properties used for these calculations are those reported for PZT-5H as listed in the Appendices A and B. These results are valid for both polar and non-polar materials.

the total energy release rate it is assumed that the crack gap does not store any energy such that the last term of Eq. (5.14) is zero. In this case the crack opening, potential drop and energy release rates are given as

$$\left.\begin{aligned} \Delta u_0 &= 4a[H_{11}\sigma + H_{12}(D-\omega_s)] \\ \Delta\phi_0 &= 4a[H_{12}\sigma + H_{22}(D-\omega_s)] \\ G^{\text{imp.}} &= G^{\text{imp.}}_{\text{tip}} = G^{\text{imp.}}_{\text{total}} = \pi a[H_{11}\sigma^2 + 2H_{12}\sigma(D-\omega_s) + H_{22}(D-\omega_s)^2] \end{aligned}\right\} \text{impermeable boundary conditions} \tag{5.29}$$

Then, for the so-called "exact" boundary conditions $D_c = -\kappa_0\Delta\phi_0/\Delta u_0$ and $\sigma_c = 0$. Also, when analyzing the total energy release rate with these boundary conditions, Eq. (5.14) with $h_c = -\kappa_0\Delta\phi_0^2/2\Delta u_0^2$ is used for Ω. Then, the crack opening, potential drop, crack tip and total energy release rates are

$$\left.\begin{aligned} \Delta u_0 &= 4a\frac{\eta_{22}\sigma - \eta_{12}(D-\omega_s) + \eta_{11}\kappa_0 - \sqrt{[\eta_{12}(D-\omega_s) - \eta_{11}\kappa_0 - \eta_{22}\sigma]^2 - 4\kappa_0\sigma(\eta_{11}\eta_{22} - \eta_{12}^2)}}{2(\eta_{11}\eta_{22} - \eta_{12}^2)} \\ \Delta\phi_0 &= \frac{4a\sigma - \eta_{11}\Delta u_0}{\eta_{12}} \\ G^{\text{exact}}_{\text{tip}} &= \pi a\left[H_{11}\sigma^2 + 2H_{12}\sigma\left(D - \omega_s + \kappa_0\frac{\Delta\phi_0}{\Delta u_0}\right) + H_{22}\left(D - \omega_s + \kappa_0\frac{\Delta\phi_0}{\Delta u_0}\right)^2\right] \\ G^{\text{exact}}_{\text{total}} &= G^{\text{exact}}_{\text{tip}} - \frac{\pi}{4}\kappa_0\frac{\Delta\phi_0^2}{\Delta u_0} \end{aligned}\right\} \text{"exact" boundary conditions} \tag{5.30}$$

Fig. 7 plots results for the energy release rates for all three models. The values for the material properties used to generate the results shown in Fig. 7 are characteristic of PZT-5H and are listed in Appendix A. Note that the total and crack tip energy release rates are equal for the impermeable and energetically consistent boundary conditions, but these two quantities differ for the "exact" boundary conditions.

Furthermore, note that the crack tip energy release rates are computed from Eq. (5.6), whereas the total energy release rates are computed from $G_{\text{total}} = -\partial\Omega/\partial(2a)$. As for Fig. 6, the results of Fig. 7 are valid for either polar or non-polar materials.

Fig. 7 illustrates a number of interesting features of this problem. First, for the modest applied stress level of 10-MPa the difference between the crack tip energy release rate and the total energy release rate for the "exact" boundary conditions that are so prevalent in the literature is significant over a wide range of $D - \omega_s$. Furthermore, the simple fact that these two quantities differ, regardless of the magnitude of the difference, is unappealing from a theoretical perspective. It is also interesting to note that both the "exact" and energetically consistent boundary conditions yield energy release rates significantly higher than the energy release rate for the impermeable boundary conditions. This feature arises because the existence of cracks in the presence of electric fields tends to be a high-energy state and hence electric fields tend to retard crack growth and the energy released during crack growth. This retardation process is maximized for the impermeable boundary conditions, but reduced for the "exact" and energetically consistent boundary conditions where electric fields can permeate through the crack gap. Finally, the energy release rate for the energetically consistent boundary conditions is higher than the total energy release rate for the "exact" boundary conditions. This result may seem counterintuitive since in addition to allowing for electric fields within the crack gap, the energetically consistent boundary conditions also include a *closing* traction on the crack faces. One would expect that the closing traction should further reduce the energy release rate. However, recall that the energetically consistent boundary conditions cause the electrical enthalpy to be stationary, and this is equivalent to minimizing the potential energy Π of the system. Recall that for the specific case of the Griffith crack problem $G_{\text{total}} = -\partial\Omega/\partial(2a) = -\partial\Pi/\partial(2a) = -\Pi/a$. Therefore, the solution that minimizes Π will maximize the total energy release rate.

One final observation from the solutions presented in Fig. 7 is that the electric field in the crack gap is much larger than the level of electric field applied to the solid. This feature of the solution, along with experimental observations of discharge in crack gaps, is the motivation to study the effects of electrical discharge on the energy release rate for this system. In order to determine if (5.27) and (5.28) yield the valid solution, the condition that the electric field in the crack gap is less than the discharge field, $|\Delta\phi_0/\Delta u_0| \leqslant E_d$, must be verified. If the solution to (5.27) and (5.28) yields $|\Delta\phi_0/\Delta u_0| > E_d$ then the solutions for the crack opening displacement, potential drop, and level of discharge are given as

$$\Delta u_0 = 4a\frac{\sigma - (D-\omega_s)\text{sgn}(\omega_d)E_d + \kappa_0 E_d^2/2}{\eta_{11} - 2\eta_{12}\text{sgn}(\omega_d)E_d + \eta_{22}E_d^2} \quad \text{if } |\omega_d| > 0 \tag{5.31}$$

$$\Delta\phi_0 = -\text{sgn}(\omega_d)E_d\Delta u_0 = -4a\text{sgn}(\omega_d)E_d\frac{\sigma - (D-\omega_s)\text{sgn}(\omega_d)E_d + \kappa_0 E_d^2/2}{\eta_{11} - 2\eta_{12}\text{sgn}(\omega_d)E_d + \eta_{22}E_d^2} \quad \text{if } |\omega_d| > 0 \tag{5.32}$$

$$\omega_d = D - \omega_s - \kappa_0\text{sgn}(\omega_d)E_d - (\eta_{12} - \eta_{22}\text{sgn}(\omega_d)E_d)\frac{\sigma - (D-\omega_s)\text{sgn}(\omega_d)E_d + \kappa_0 E_d^2/2}{\eta_{11} - 2\eta_{12}\text{sgn}(\omega_d)E_d + \eta_{22}E_d^2} \quad \text{if } |\omega_d| > 0 \tag{5.33}$$

Eq. (5.33) can be used to check the consistency for the choice of $\text{sgn}(\omega_d)$. If neither $\text{sgn}(\omega_d) = 1$ nor $\text{sgn}(\omega_d) = -1$ is consistent with Eq. (5.33) then this most likely implies the electric field in the gap is less than the critical discharge field and Eqs. (5.27) and (5.28) should be used for the solution. However, a second scenario can arise if the magnitude of the discharge field is greater than either the positive or negative critical levels defined by

$$E_d^{\text{crit}\pm} = \left|\frac{-H_{12} \pm \sqrt{H_{12}^2 - H_{11}H_{22}}}{H_{11}}\right| \tag{5.34}$$

If the discharge field is greater than the appropriate critical level then consistent solutions for the crack opening and electric displacement within the crack cannot be obtained when the electric field within the crack reaches the discharge level. The most likely physical interpretation is that the system is unstable when the electric field within the crack attains the discharge level. For the remainder of this section it will be assumed that the discharge field is less than both of the critical levels from (5.34).

Fig. 8 plots the results for the energy release rate versus the applied electric displacement for the energetically consistent boundary conditions for an applied stress level of 20-MPa and various levels of the discharge field E_{d}. For a given level of E_{d} there exists a range of applied electric displacement values that do not cause discharge, and the solution to the problem requires the solution of Eqs. (5.27) and (5.28). As the magnitude of the applied electric displacement is increased electrical discharge will eventually occur. Under these conditions Eqs. (5.31)–(5.33) provide the relevant solution and these solutions can be located on Fig. 8 as curves that branch off from the central non-discharging solution.

The most significant observation illustrated on Fig. 8 is that electric discharge tends to reduce the retarding effects of electric field, thereby increasing the energy release rate. Also, note on Fig. 8 that solutions for the energy release rate during electrical discharge drop smoothly and continuously to zero. Eqs. (5.31) and (5.33) yield interesting information about this behavior. For simplicity, consider positive applied electric displacements that cause positive electric fields within the crack. One possible way to attain an energy release rate of zero is if both the stress and electric displacement within the crack are equal to σ and $D-\omega_{\mathrm{s}}$ respectively. If this is the case then the crack opening displacement must vanish. If $\Delta u_0 = 0$, Eqs. (5.31) and (5.33) imply that the level of applied electric displacement that closes the crack, D_{closure} and the corresponding level of transferred charge are

$$D_{\mathrm{closure}} - \omega_{\mathrm{s}} = \frac{\sigma}{E_{\mathrm{d}}} + \frac{1}{2}\kappa_0 E_{\mathrm{d}} \tag{5.35}$$

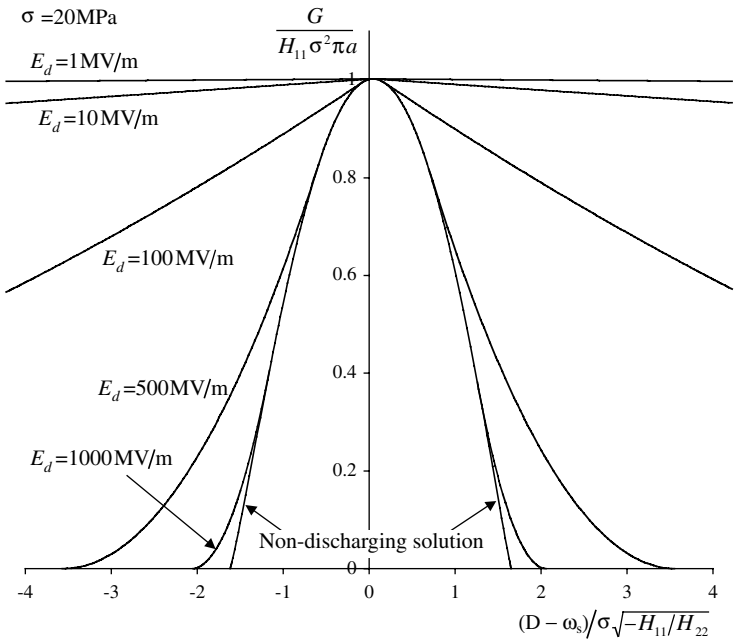

Fig. 8. The effects of electrical discharge within the crack on the energy release rate.

$$\omega_{\mathrm{d}} = D_{\mathrm{closure}} - \omega_{\mathrm{s}} - \kappa_0 E_{\mathrm{d}} = \frac{\sigma}{E_{\mathrm{d}}} - \frac{1}{2}\kappa_0 E_{\mathrm{d}} \tag{5.36}$$

Then, it is readily shown that

$$D_{\mathrm{c}} = \omega_{\mathrm{d}} + \kappa_0 E_{\mathrm{d}} = \frac{\sigma}{E_{\mathrm{d}}} + \frac{1}{2}\kappa_0 E_{\mathrm{d}} = D_{\mathrm{closure}} - \omega_{\mathrm{s}} \tag{5.37}$$

and

$$\sigma_{\mathrm{c}} = D_{\mathrm{c}} E_{\mathrm{d}} - \frac{1}{2}\kappa_0 E_{\mathrm{d}}^2 = \sigma + \frac{1}{2}\kappa_0 E_{\mathrm{d}}^2 - \frac{1}{2}\kappa_0 E_{\mathrm{d}}^2 = \sigma \tag{5.38}$$

Therefore, if the crack is closed then the stress and electric displacement within the gap are equal to the associated applied levels. Finally, applying Eq. (5.23) or (5.26) it can be shown that $G = 0$ under these conditions. Hence, the level of effective electric displacement where the energy release rate is zero corresponds to the point where the crack is closed. Levels of effective electric displacement higher than the closure level given in Eq. (5.35) only act to close the crack further. Therefore, since the crack cannot physically be closed beyond $\Delta u_0 = 0$, this electrical discharging crack model cannot lead to negative energy release rates if the discharge field is less than the critical values given in Eq. (5.34).

6. Discussion

This work has been motivated primarily by McMeeking's observation, McMeeking (2004), that the so-called "exact" electrical boundary conditions that are prevalent in the literature give rise to a discrepancy between the total and crack tip energy release rates in a cracked piezoelectric body. Such a discrepancy is objectionable from a theoretical perspective. To address this problem, energetically consistent electromechanical boundary conditions for cracks were derived in Section 3. These boundary conditions were derived based on the following assumptions. (1) The energy of the cracked body can be computed using its undeformed configuration. (2) When the crack opens electric fields can permeate the crack medium and electrical energy can be stored within the crack. (3) The energy stored within the crack medium can be computed from the deformed configuration of the cracked body. (4) Electric field components within the crack medium parallel to the crack faces are negligible compared to the electric field normal to the crack. Evidently, assumptions (1) and (3) are in contradiction with one another since the analysis of energies is mixed between deformed and undeformed configurations. However, these assumptions are consistent with those used for the "exact" boundary conditions. Furthermore, a proper resolution to this inconsistency would require a full non-linear, large deformation kinematics analysis of the problem. Instead, in this work, assumptions (1)–(4) are taken as a starting point and the energetically consistent crack boundary conditions are derived by equating the weak statements of two boundary value problems; one which models the volume of the crack gap explicitly and one that models the crack gap through the surface tractions and charges that it applies to the cracked solid.

The primary results of this paper are the energetically consistent boundary conditions given by Eqs. (3.11)–(3.14). These boundary conditions imply that cracks in electromechanical materials not only sustain electric field and electric displacement, but also apply mechanical traction to the surrounding material. This feature of mechanical forces arising due to electrical effects is common in finite deformation analyses of electromechanical materials and is usually termed a Maxwell stress. With these energetically consistent boundary conditions, Section 4 was used to demonstrate that a small modification to the J-integral could be used to compute the energy release rate for crack advance in a non-linear but reversible electromechanical solid. The results of Sections 3 and 4 will be especially useful for the analysis of cracked piezoelectric bodies with the finite element method. McMeeking (1999) and Gruebner et al. (2003) have already implemented

the finite element method with the "exact" boundary conditions. Similar computations can readily be performed with the new energetically consistent boundary conditions and the modified J-integral of Section 4 can be used to determine the energy release rate within these types of calculations. Finally, in Section 5, the specific example of a Griffith crack in a poled linear piezoelectric solid was used to demonstrate that the energetically consistent boundary conditions do in fact resolve the discrepancy between the crack tip and total energy release rates. Furthermore, the effects of electrical discharge on the energy release rate was ascertained and shown to reduce the retarding effects of electric fields on crack growth.

Acknowledgement

The author would like to acknowledge support for this work from the National Science Foundation through grant number CMS-0238522.

Appendix A

The treatment of the Griffith crack problem outlined in Section 5 assumes that the components of the Irwin matrix for the material are known. Irwin matrices are given in this appendix for PZT-5H as reported by McMeeking (2004) and for materials with a special form of simplified piezoelectric properties as given by Landis (2004).

For PZT-5H, McMeeking (2004) reports the following piezoelectric coefficients for a material that is poled and transversely isotropic about the x_3-axis.

$$c^E_{1111} = 126 \text{ GPa}, \quad c^E_{1122} = 55 \text{ GPa}, \quad c^E_{1133} = 53 \text{ GPa}, \quad c^E_{3333} = 117 \text{ GPa}, \quad c^E_{2323} = 35.3 \text{ GPa}$$

$$e_{311} = -6.5 \text{ C/m}^2, \quad e_{333} = 23.3 \text{ C/m}^2, \quad e_{113} = 17 \text{ C/m}^2$$

$$\kappa^\varepsilon_{11} = 15.1 \times 10^{-9} \text{ C/V m}, \quad \kappa^\varepsilon_{33} = 13 \times 10^{-9} \text{ C/V m}$$

Then, the Irwin matrix for PZT-5H poled in the x_2 direction under plane strain conditions is

$$\begin{bmatrix} H_{11} & H_{12} \\ H_{12} & H_{22} \end{bmatrix} = \begin{bmatrix} 0.803 \times 10^{-11} \text{ m}^2/\text{N} & 0.639 \times 10^{-3} \text{ m}^2/\text{C} \\ 0.639 \times 10^{-3} \text{ m}^2/\text{C} & -2.289 \times 10^{7} \text{ V m/C} \end{bmatrix} \tag{A.1}$$

Of course, this result for the Irwin matrix is applicable only to PZT-5H, and in order to obtain results for a different material the associated Irwin matrix needs to be determined. This can be accomplished by following the procedure described by McMeeking (2004) among others. On the other hand, if the material properties can be reasonably approximated with the following description due to Landis (2004) then the Irwin matrix can be obtained in closed form.

Specifically, if the elastic compliance and dielectric permittivity tensors can be assumed to be isotropic and the piezoelectric d coefficients satisfy transversely isotropic symmetries and $d_{113} = (d_{333} - d_{311})/2$, then the non-zero strain and electric displacement components due to electromechanical loading in the 1–3 plane for a material poled in the x_3 direction are given as

$$\varepsilon_{11} = \frac{1}{E}\sigma_{11} - \frac{v}{E}\sigma_{22} - \frac{v}{E}\sigma_{33} + d_{311}E_3 \tag{A.2}$$

$$\varepsilon_{22} = -\frac{v}{E}\sigma_{11} + \frac{1}{E}\sigma_{22} - \frac{v}{E}\sigma_{33} + d_{311}E_3 \tag{A.3}$$

$$\varepsilon_{33} = -\frac{v}{E}\sigma_{11} - \frac{v}{E}\sigma_{22} + \frac{1}{E}\sigma_{33} + d_{333}E_3 \tag{A.4}$$

$$\varepsilon_{13} = \frac{1+v}{E}\sigma_{13} + \frac{d_{333}-d_{311}}{2}E_1 \tag{A.5}$$

$$D_1 = (d_{333}-d_{311})\sigma_{13} + \kappa E_1 \tag{A.6}$$

$$D_3 = d_{311}\sigma_{11} + d_{311}\sigma_{22} + d_{333}\sigma_{33} + \kappa E_3 + P_3^r \tag{A.7}$$

Here E and v are the isotropic Young's modulus and Poisson's ratio at constant electric field, κ is the isotropic dielectric permittivity at constant stress, and d_{333} and d_{333} are piezoelectric coefficients. Then, the Irwin matrix for such a material poled in the x_2 direction in plane strain is

$$\begin{bmatrix} H_{11} & H_{12} \\ H_{12} & H_{22} \end{bmatrix} = \left[\begin{array}{c|c} \frac{-k_\varepsilon}{4\mathscr{D}_D}\left\{\left(\frac{d_{15}}{d_{31}}\right)^2\frac{\mathscr{D}_E}{1+v} + 8\left[\alpha_\varepsilon\left(\frac{d_{15}}{d_{31}}\right) - \frac{d_{33}}{d_{31}}\right]\right\}\frac{1-v^2}{E} & \frac{1}{2\mathscr{D}_D}\left[\left(\frac{d_{15}}{d_{31}}\right)\mathscr{D}_E + 4(\alpha_\varepsilon - 1)(1+v)\right]\frac{d_{31}}{\kappa} \\ \hline \frac{1}{2\mathscr{D}_D}\left[\left(\frac{d_{15}}{d_{31}}\right)\mathscr{D}_E + 4(\alpha_\varepsilon - 1)(1+v)\right]\frac{d_{31}}{\kappa} & -\frac{\mathscr{D}_E}{\mathscr{D}_D}\frac{1}{2\kappa} \end{array}\right] \tag{A.8}$$

where $d_{33} = d_{333}$, $d_{31} = d_{311}$, $d_{15} = d_{333} - d_{311}$,

$$\mathscr{D}_{\mathrm{D}} = k_\varepsilon(1-v) + 2(\alpha_\varepsilon - 1)(1+v), \quad \mathscr{D}_E = k_\varepsilon\alpha_\varepsilon(1-v) + 2(\alpha_\varepsilon - 1)(1+v),$$

$$k_\varepsilon = \frac{2Ed_{31}^2}{\kappa(1-v)} \quad \text{and} \quad \alpha_\varepsilon = \sqrt{\frac{1}{1-k_\varepsilon}}.$$

For plane stress the Irwin matrix for this material is

$$\begin{bmatrix} H_{11} & H_{12} \\ H_{12} & H_{22} \end{bmatrix} = \left[\begin{array}{c|c} \frac{k_\sigma}{2}\left[\frac{\alpha_\sigma}{\alpha_\sigma - 1} - \left(\frac{d_{33}}{d_{31}}\right)^2\right]\frac{1}{E} & \frac{d_{33}}{2\kappa} \\ \hline \frac{d_{33}}{2\kappa} & -\frac{1}{2\kappa} \end{array}\right] \tag{A.9}$$

where $k_\sigma = \frac{Ed_{31}^2}{\kappa}$ and $\alpha_\sigma = \sqrt{\frac{1}{1-k_\sigma}}$.

Appendix B

In this appendix the effects of the energetically consistent boundary conditions on the first two terms of the asymptotic expansion for the solutions near crack tips in linear piezoelectric solids are outlined. It is expected that the non-singular T terms will have an effect on the sizes and shapes of switching zones near crack tips in non-linear ferroelectric materials. As in Section 5 simplicity is sought by considering only mixed Modes I and D loading. The inclusion of Modes II and III would require additional singular K terms, but the non-singular T terms would remain unchanged. Under mixed Mode I and Mode D the Cartesian components of the stresses and electric displacements near a crack tip in a linear piezoelectric solid can be expanded into the forms

$$\sigma_{ij}(r,\theta) = \frac{K_{\mathrm{I}}}{\sqrt{2\pi r}}\tilde{\sigma}_{ij}^I(\theta) + \frac{K_{\mathrm{D}}}{\sqrt{2\pi r}}\tilde{\sigma}_{ij}^D(\theta) + T_{ij}^\sigma + O(\sqrt{r}) \tag{B.1}$$

$$D_i(r,\theta) = \frac{K_{\mathrm{I}}}{\sqrt{2\pi r}}\tilde{D}_i^I(\theta) + \frac{K_{\mathrm{D}}}{\sqrt{2\pi r}}\tilde{D}_i^D(\theta) + T_i^D + O(\sqrt{r}) \tag{B.2}$$

Here r and θ are polar coordinates as illustrated in Fig. 2, and $\tilde{\sigma}^I_{ij}(\theta) = \tilde{\sigma}^I_{ji}(\theta)$, $\tilde{\sigma}^D_{ij}(\theta) = \tilde{\sigma}^D_{ji}(\theta)$, $\tilde{D}^I_i(\theta)$ and $\tilde{D}^D_i(\theta)$ are dimensionless functions of θ that satisfy the following boundary conditions,

$$\tilde{\sigma}^I_{22}(\theta = 0) = \tilde{D}^D_2(\theta = 0) = 1 \tag{B.3}$$

$$\tilde{\sigma}^D_{22}(\theta = 0) = \tilde{\sigma}^I_{12}(\theta = 0) = \tilde{\sigma}^D_{12}(\theta = 0) = \tilde{\sigma}^I_{23}(\theta = 0) = \tilde{\sigma}^D_{23}(\theta = 0) = \tilde{D}^I_2(\theta = 0) = 0 \tag{B.4}$$

$$\tilde{\sigma}^I_{22}(\theta = \pm\pi) = \tilde{\sigma}^I_{12}(\theta = \pm\pi) = \tilde{\sigma}^I_{23}(\theta = \pm\pi) = \tilde{D}^D_2(\theta = \pm\pi) = 0 \tag{B.5}$$

$$\tilde{\sigma}^D_{22}(\theta = \pm\pi) = \tilde{\sigma}^D_{12}(\theta = \pm\pi) = \tilde{\sigma}^D_{23}(\theta = \pm\pi) = \tilde{D}^I_2(\theta = \pm\pi) = 0 \tag{B.6}$$

Notice that the boundary conditions represented by Eqs. (B.5) and (B.6) are the same as those associated with the impermeable crack model. Hence, the impermeable crack boundary conditions are valid for the singular K terms, and standard methods can be applied to determine the dimensionless stress and electric displacement functions, e.g. Suo et al. (1992).

The direct effects of the energetically consistent boundary conditions first arise in the non-singular T terms. Near the crack tip the jumps in displacement and electric potential across the crack are given as

$$\Delta u_2 = u_2(r, \theta = \pi) - u_2(r, \theta = -\pi) = 4\sqrt{\frac{2r}{\pi}}(H_{11}K_{\mathrm{I}} + H_{12}K_{\mathrm{D}}) + O(r^{3/2}) \tag{B.7}$$

$$\Delta\phi = \phi(r, \theta = \pi) - \phi(r, \theta = -\pi) = 4\sqrt{\frac{2r}{\pi}}(H_{12}K_{\mathrm{I}} + H_{22}K_{\mathrm{D}}) + O(r^{3/2}) \tag{B.8}$$

where the H terms are the components of the Irwin matrix as given in Appendix A. Then the electric field in the crack gap is given as

$$E_{\mathrm{c}} = -\frac{\Delta\phi}{\Delta u_2} = -\frac{H_{11}K_{\mathrm{I}} + H_{12}K_{\mathrm{D}}}{H_{12}K_{\mathrm{I}} + H_{22}K_{\mathrm{D}}} + O(r) \tag{B.9}$$

which is independent of r to leading order near the crack tip. This implies that the electric displacement and the stress acting through the crack gap are constant to leading order near the crack tip as well and are given by

$$D_{\mathrm{c}} = -\frac{\mathrm{d}h_{\mathrm{c}}}{\mathrm{d}E_{\mathrm{c}}} \quad \text{and} \quad \sigma_{\mathrm{c}} = h_{\mathrm{c}} + E_{\mathrm{c}}D_{\mathrm{c}} \tag{B.10}$$

Then, in order to satisfy the energetically consistent boundary conditions, the T terms must satisfy the conditions

$$T^\sigma_{22} = \sigma_{\mathrm{c}}, \quad T^D_2 = D_{\mathrm{c}}, \quad \text{and} \quad T^\sigma_{12} = T^\sigma_{21} = T^\sigma_{23} = T^\sigma_{32} = 0 \tag{B.11}$$

The remaining terms T^σ_{11}, T^σ_{33}, $T^\sigma_{13} = T^\sigma_{31}$, T^D_1 and T^D_3 take on values as determined from the geometry of the cracked body and the applied electromechanical loading.

Finally, it is important to note that there is a coupling between the singular K terms and the non-singular T terms when applying the energetically consistent boundary conditions. Specifically, the dependence of T^σ_{22} and T^D_2 on K_{I} and K_{D} is demonstrated by Eqs. (B.9)–(B.11), whereas K_{I} and K_{D} depend on T^σ_{22} and T^D_2 (i.e. σ_{c} and D_{c}) through the details of the boundary value problem as illustrated for the Griffith crack problem in Eqs. (5.21) and (5.22).

References

Chen, Y.-H., Lu, T.J., 2002. Cracks and fracture in piezoelectrics. Adv. Appl. Mech. 39, 121–215.
Deeg, W.F., 1980. The analysis of dislocation, crack and inclusion problems in piezoelectric solids. Ph.D. Thesis, Stanford University.
Gruebner, O., Kamlah, M., Munz, D., 2003. Finite element analysis of cracks in piezoelectrics taking into account the permittivity of the crack medium. Eng. Fract. Mech. 70, 1399–1413.
Hao, T.-H., Shen, Z.-Y., 1994. A new electric boundary condition of electric fracture mechanics and its application. Eng. Fract. Mech. 47, 793–802.
Landis, C.M., 2004. In-plane complex potentials for a special class of materials with degenerate material properties. Int. J. Solids Struct. 41, 695–715.
Landis, C.M., McMeeking, R.M., 2000. Modeling of fracture in ferroelectric ceramics. Proc. SPIE 3992, 176–184.
Li, J.C.M., Ting, T.W., 1957. Thermodynamics for elastic solids in the electrostatic field. I. General formulation. J. Chem. Phys. 27, 693–700.
McMeeking, R.M., 1999. Crack tip energy release rate for a piezoelectric compact tension specimen. Eng. Fract. Mech. 64, 217–244.
McMeeking, R.M., 2004. The energy release rate for a Griffith crack in a piezoelectric material. Eng. Fract. Mech. 71, 1149–1163.
Pak, Y.E., 1992. Linear electro-elastic fracture mechanics of piezoelectric materials. Int. J. Fract. 54, 79–100.
Parton, V.Z., 1976. Fracture mechanics of piezoelectric materials. Acta Astronautica 3, 671–683.
Sosa, H., 1992. On the fracture mechanics of piezoelectric solids. Int. J. Solids Struct. 29, 2613–2622.
Sosa, H., Khutoryansky, N., 1996. New developments concerning piezoelectric materials with defects. Int. J. Solids Struct. 33, 3399–3414.
Suo, Z., Kuo, C.M., Barnett, D.M., Willis, J.R., 1992. Fracture mechanics for piezoelectric ceramics. J. Mech. Phys. Solids 40, 739–765.
Xu, X.L., Rajapakse, R.K.N.D., 2001. On a plane crack in piezoelectric solids. Int. J. Solids Struct. 38, 7643–7658.
Zhang, T.Y., Gao, C.F., 2004. Fracture behaviors of piezoelectric materials. Theor. Appl. Fract. Mech. 41, 339–379.
Zhang, T.-Y., Zhao, M., Tong, P., 2001. Fracture of piezoelectric ceramics. Adv. Appl. Mech. 38, 147–289.

Available online at www.sciencedirect.com
SCIENCE DIRECT®
International Journal of Solids and Structures 42 (2005) 2461–2463
INTERNATIONAL JOURNAL OF SOLIDS and STRUCTURES
www.elsevier.com/locate/ijsolstr

Corrigendum

Energetically consistent boundary conditions for electromechanical fracture [International Journal of Solids and Structures 41 (2004) 6291–6315]

Chad M. Landis *

Mechanical Engineering and Materials Science, P.O. Box 1892, Houston, TX 77251 1892, United States

Received 9 August 2004
Available online 27 October 2004

The author regrets a transcription error in a quantity used for the numerical results presented in Figs. 6–8. Eq. (A.1) of Appendix A reports that the Irwin matrix for PZT-5H poled in the x_2 direction under plane strain conditions is

$$\begin{bmatrix} H_{11} & H_{12} \\ H_{12} & H_{22} \end{bmatrix} = \begin{bmatrix} 0.803\times10^{-11}\,\mathrm{m^2/N} & 0.639\times10^{-3}\,\mathrm{m^2/C} \\ 0.639\times10^{-3}\,\mathrm{m^2/C} & -2.289\times10^{7}\,\mathrm{V\,m/C} \end{bmatrix} (\text{Incorrect for PZT}-5\text{H}) \tag{A.1}$$

where the material properties (if poled in the x_3 direction) used to derive this matrix are

$$c^E_{1111} = 126\,\mathrm{GPa},\quad c^E_{1122} = 55\,\mathrm{GPa},\quad c^E_{1133} = 53\,\mathrm{GPa},\quad c^E_{3333} = 117\,\mathrm{GPa},\quad c^E_{2323} = 35.3\,\mathrm{GPa}$$
$$e_{311} = -6.5\,\mathrm{C/m^2},\quad e_{333} = 23.3\,\mathrm{C/m^2},\quad e_{113} = 17\,\mathrm{C/m^2}$$
$$\kappa^{\varepsilon}_{11} = 15.1\times10^{-9}\,\mathrm{C/V\,m},\quad \kappa^{\varepsilon}_{33} = 13\times10^{-9}\ \mathrm{C/V\,m}$$

The error occurs in the H_{12} term, which should be 6.39×10^{-3} instead of 0.639×10^{-3}. Hence the correct Irwin matrix for PZT-5H is

$$\begin{bmatrix} H_{11} & H_{12} \\ H_{12} & H_{22} \end{bmatrix} = \begin{bmatrix} 0.803\times10^{-11}\,\mathrm{m^2/N} & 6.39\times10^{-3}\,\mathrm{m^2/C} \\ 6.39\times10^{-3}\,\mathrm{m^2/C} & -2.289\times10^{7}\,\mathrm{V\,m/C} \end{bmatrix} (\text{Correct for PZT}-5\text{H}) \tag{A.1}$$

The corrected numerical results presented in Figs. 6–8 are as follows. Note that the qualitative discussion of each of these figures is unaffected by this error.

Note that a publishing error occurred in the original Fig. 7. Minus signs are missing on the exponents in the H_{11} and H_{12} terms appearing on the figure inset, and an "×" does not appear prior to the 10's.

DOI of original article 10.1016/j.ijsolstr.2004.05.062.
* Tel.: +1 713 3483 609; fax: +1 713 3485 423.
E-mail address: landis@rice.edu

0020-7683/$ - see front matter
doi:10.1016/j.ijsolstr.2004.09.017

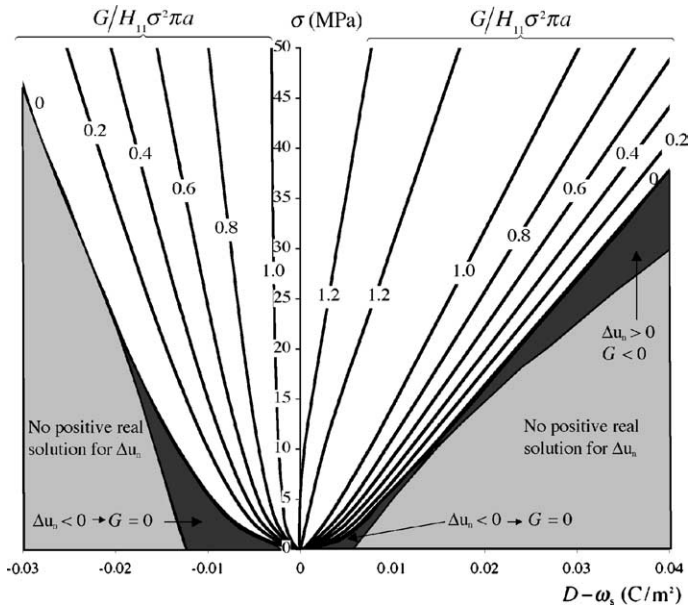

Fig. 6. A contour plot of normalized energy release rate G (total or crack tip) for a remotely loaded Griffith crack versus applied stress and applied effective electric displacement. Energetically consistent boundary conditions with no discharge allowed are applied to generate this solution. The material is linear piezoelectric with properties characteristic of PZT-5H and the Irwin matrix as corrected above.

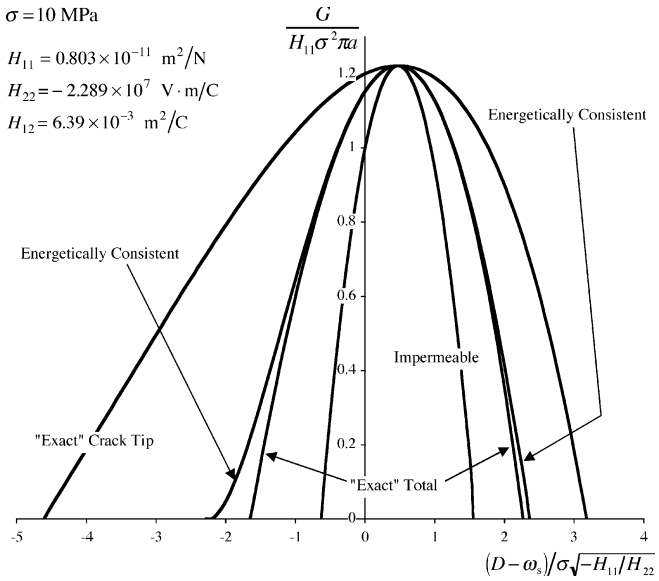

Fig. 7. Energy release rates for a Griffith crack in a linear piezoelectric solid with no discharge in the crack allowed. The properties used for these calculations are those reported for PZT-5H and the Irwin matrix as corrected above. These results are valid for both polar and non-polar materials.

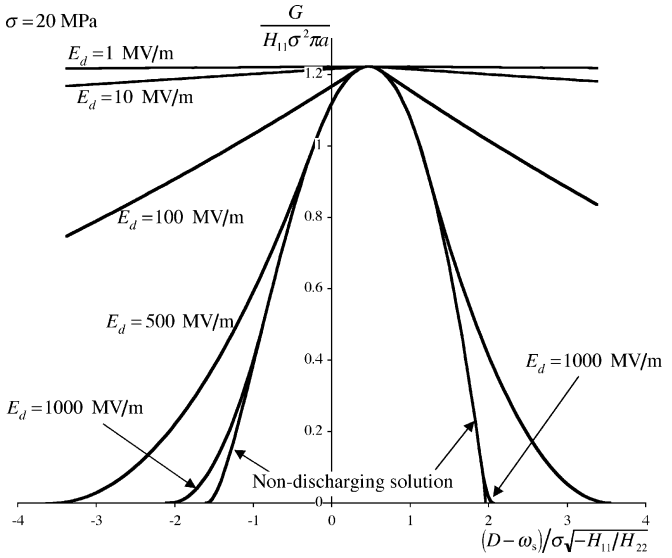

Fig. 8. The effects of electrical discharge within the crack on the energy release rate. Results are reported only for the energetically consistent boundary conditions. The properties used for these calculations are those reported for PZT-5H and the Irwin matrix as corrected above.

Finally, the results presented in the original manuscript are in fact valid for a material with the Irwin matrix as first reported. However, such an Irwin matrix does not result from the material properties for PZT-5H as reported in the manuscript and above. One set of material properties that does yield this original Irwin matrix to within 0.2% for each term is

$$c^E_{1111} = c^E_{3333} = 152.1\,\text{GPa}, \quad c^E_{1122} = c^E_{1133} = 65.19\,\text{GPa}, \quad c^E_{2323} = 43.46\ \text{GPa}$$
$$e_{311} = -1.428\,\text{C/m}^2, \quad e_{333} = 2.855\,\text{C/m}^2, \quad e_{113} = 2.142\,\text{C/m}^2$$
$$\kappa^{\varepsilon}_{11} = 21.75 \times 10^{-9}\,\text{C/V m}, \quad \kappa^{\varepsilon}_{33} = 21.79 \times 10^{-9}\,\text{C/V m}$$

Hence, the originally reported results are valid for such a piezoelectric material.

The author sincerely apologizes for any confusion or difficulties this error may have caused.